ELSEVIER

Computational Materials Science 31 (2004) 33–41

COMPUTATIONAL MATERIALS SCIENCE

www.elsevier.com/locate/commatsci

Metallic–semiconducting transition of single-walled carbon nanotubes under high axial strain

Yoshitaka Umeno *, Takayuki Kitamura, Akihiro Kushima

Department of Engineering Physics and Mechanics, Graduate School of Engineering, Kyoto University, Yoshida-hommachi, Sakyo-ku, Kyoto-shi, Kyoto 606-8501, Japan

Received 12 August 2003; received in revised form 18 November 2003; accepted 14 January 2004

Abstract

Carbon nanotubes (CNTs) have been attracting attention because of their characteristic mechanical and electronic properties. It has been pointed out that a single-walled CNT can stretch in the axial direction at 30% strain without any bonds breaking. Therefore, it is of interest to investigate electronic properties of CNTs under high axial strain. In this study, we investigate the change in electronic properties of single-walled CNTs under high axial strain with tight-binding semiempirical band calculations. The property of CNTs with the chiral vectors, (m, n); $m - n = 3q$, where m, n and q are integers, shows the transition, metallic $\rightarrow$ semiconducting $\rightarrow$ metallic in that order under tension, except armchair tubes, which remain metallic. The transition in CNTs with the chiral vectors of $m - n = 3q + 1$ or $m - n = 3q + 2$ is: semiconducting $\rightarrow$ metallic $\rightarrow$ semiconducting, and the transient strain is dependent on the diameter of the CNTs.

PACS: 31.15.Ct; 61.46.+w; 62.25.+g; 73.22.−f
Keywords: Carbon nanotube; Tight-binding; Simulation; Electronic property; Strain; Deformation

1. Introduction

Development of microscopic processing technology in recent years has stimulated attempts to manufacture small components with arranged structures at the nanometer scale. One particular example is carbon nanotubes (CNTs), which were discovered by Iijima [1,2], and are nanomaterials constructed by covalent bonds of carbon atoms. They have attracted attention for application to electronic nanodevices because of their structural stability and prominent electronic properties. It is important to clarify the mechanical and electronic properties of CNTs for the relevant applications.

The electronic structure of CNTs has been studied in detail [3–10] and its change under low strain has been investigated [11–14]. Furthermore, experiments and numerical simulations have been carried out on the mechanical deformation of CNTs, highlighting some eccentric properties [15–27]. For example, a single-walled CNT can stretch

* Corresponding author. Tel./fax: +81-75-753-5256.
E-mail address: umeno@kues.kyoto-u.ac.jp (Y. Umeno).
URL: http://cyber.kues.kyoto-u.ac.jp.

0927-0256/$ - see front matter © 2004 Elsevier B.V. All rights reserved.
doi:10.1016/j.commatsci.2004.01.033

in the axial direction by more than 30% of axial strain depending on conditions of temperature and strain rate without any bonds breaking [28]. These results indicate that investigating electronic properties under high axial strain is of importance.

In this study, we conduct tight-binding semi-empirical band calculations to evaluate change in the electronic properties of single-walled CNTs under high axial strain after verifying the validity of the method by ab initio calculations.

2. Calculation method of electronic structure

2.1. Ab initio calculation

According to the density functional theory (DFT) [29], the total energy of a system, E, is expressed as a functional of the charge density, ρ,

$$E[\rho] = T[\rho] + \int V_{\text{ext}}(\mathbf{r})\rho(\mathbf{r})\,\mathrm{d}\mathbf{r} + \frac{1}{2}\int\int \frac{\rho(\mathbf{r}')\rho(\mathbf{r})}{|\mathbf{r}'-\mathbf{r}|}\,\mathrm{d}\mathbf{r}'\,\mathrm{d}\mathbf{r} + E_{\text{xc}}[\rho]. \quad (1)$$

Here, $\mathbf{r}$ indicates the coordinate vector in the real space, and the terms on the right-hand side are the kinetic energy of electrons, the potential energy of electrons induced by nuclei, the coulomb interaction between electrons, and the exchange-correlation energy of electrons, respectively. Under the local density approximation, the solution of Eq. (1) is obtained by solving the one-electron Schrödinger equation (the Kohn–Sham equation) [30],

$$H\psi_i = E\psi_i, \quad (2)$$

where i indicates the electron state, ψ is the wave function, and $H = -\frac{1}{2}\nabla^2 + V$. Since V includes the potential acting on the electron, which is a functional of the charge density, ρ,

$$\rho(\mathbf{r}) = \sum_i |\psi_i(\mathbf{r})|^2, \quad (3)$$

where the sum runs over all the occupied states, the above equations should be solved self-consistently.

2.2. Tight-binding calculation

In a tight-binding calculation, the Schrödinger equation is solved in a simplified process, briefly explained below, so that computational time is greatly reduced in comparison with the ab initio method. The hamiltonian is constructed with the effective potential, V,

$$H = -\frac{1}{2}\nabla^2 + V, \quad (4)$$

where the first term on the right-hand side represents the kinetic energy, and V is obtained by simple functions with parameters (TB potential). The wave functions are expressed as linear combinations of atomic orbitals (LCAO) [31,32]. The hamiltonian is solved once and no self-consistent iteration is performed.

3. Validity of tight-binding calculation

3.1. Simulation procedure

To verify the accuracy of the tight-binding calculation method, the atomic configuration and the electronic structure of an (8,8) armchair CNT and a (9,0) zigzag CNT are evaluated by the ab initio and the tight-binding molecular dynamics simulations.

Fig. 1 shows the simulation cells for the (8,8) and the (9,0) tubes, which contain 32 and 36 atoms, respectively. The norm conserving pseudopotential method using a plane wave basis set is adopted for the ab initio calculation, with which molecular dynamics simulations can be easily carried out [30,33,34]. The efficient pseudopotential suggested by Troullier and Martins [35] is used and the cut-off energy of plane waves is set to be 50.0 Ry. The exchange-correlation energy is evaluated using the function suggested by Ceperley and Alder [36] based on the local density approximation (LDA) [37], and the wave functions are converged by the RMM-DIIS optimization algorithm [38] with parallel computation. Because periodic boundary conditions are imposed in every direction, the sizes of the simulation cell in the x and y directions (L_x and L_y) has to be large enough. In the ab initio calculations, L_x and L_y are larger than $d + 6$ Å, where d is the diameter of the tube. We have verified that this is large enough to eliminate the effect of neighboring CNTs by calculations using a larger cell (L_x and $L_y > 10d$). 25 $\boldsymbol{k}$-points are selected for

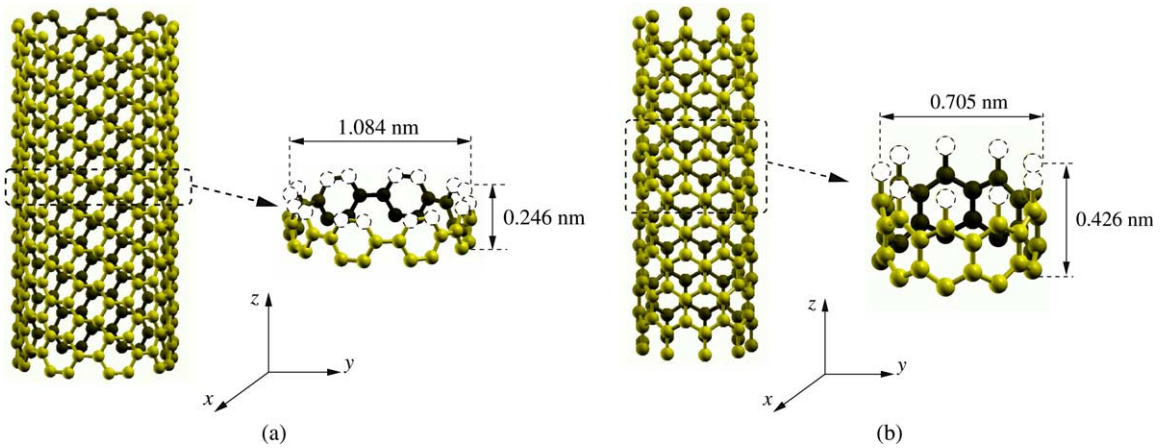

Fig. 1. Simulation models of (a) (8,8) and (b) (9,0) CNTs.

the (8,8) tube and 30 for the (9,0) tube for obtaining band structures along the z direction. The convergence is also confirmed by a preliminary calculation with different number of $\boldsymbol{k}$-points.

Under the TB method, the two potentials proposed by Papaconstantopoulos and coworker [39] and Wang and co workers [40] are adopted for comparison. The relaxation of the atomic configuration is accelerated by removing the kinetic energy of the atoms at certain steps in both the calculations. 50 $\boldsymbol{k}$-points along the z direction are selected in the TB calculations.

We also examined the validity of the TB method for evaluating the electronic properties of CNTs under tension. The strain in the z direction, $\varepsilon = 0.20$, is applied to the cell shown in Fig. 1, and the atom configuration is relaxed. Then, the band structure is evaluated by the TB and ab initio calculations.

3.2. Results and discussions

Fig. 2(a) shows the band structure of the (8,8) armchair CNT at $\varepsilon = 0$, evaluated by the ab initio method and the TB method proposed by Papaconstantpoulos. The results agree closely with each other, which means that the TB potential used for the simulations is suitable for evaluating the electronic property of CNTs. On the other hand, the

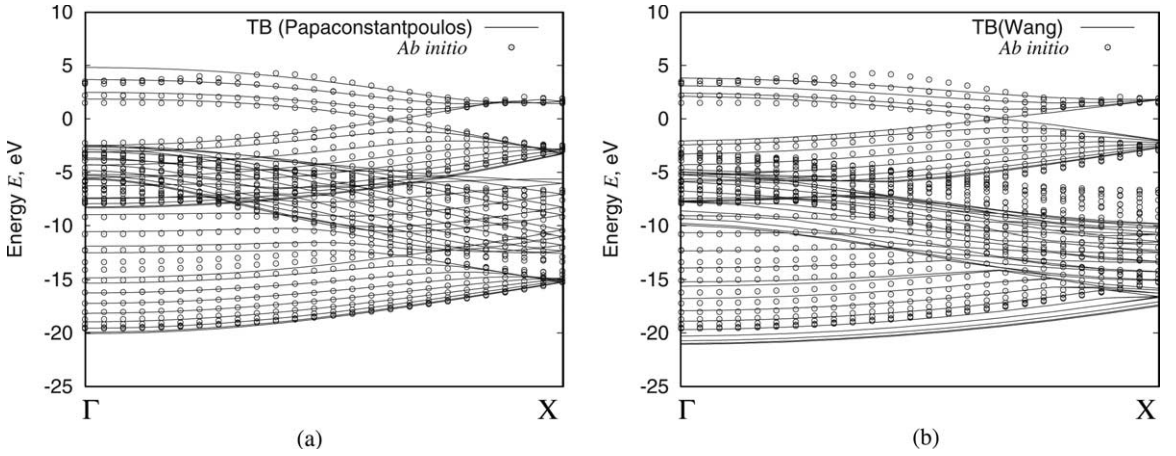

Fig. 2. Band structure of (8,8) armchair CNT without tension.

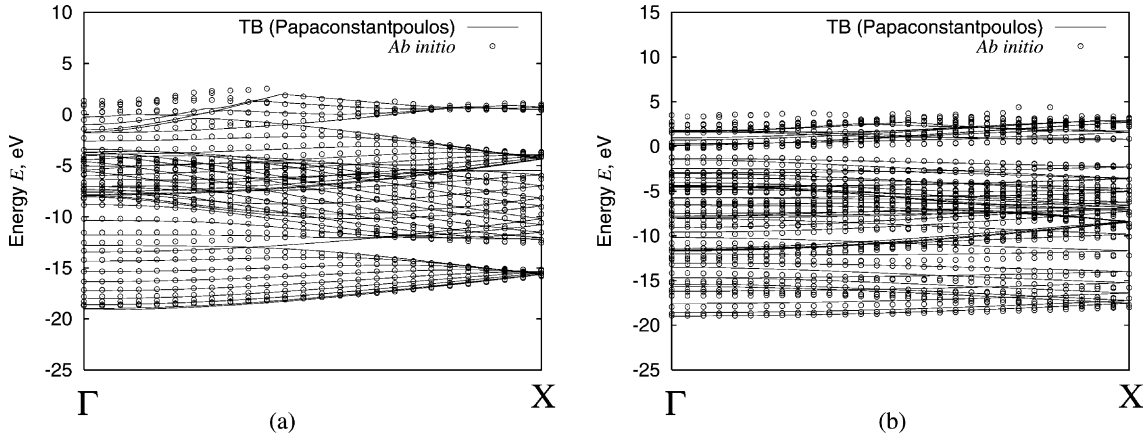

Fig. 3. Band structure of (8,8) and (9,0) CNTs under tension ($\varepsilon = 0.2$). (a) (8,8) tube and (b) (9,0) tube.

band structure obtained by the Wang TB potential (Fig. 2(b)) is conspicuously different to that by the ab initio simulation. Blase et al. [8] have also pointed out that TB calculations can cause errors in terms of evaluating the electronic properties of CNTs. These results indicate that the validity on evaluation of band structure depends on the TB potential and that a suitable TB potential should be selected in calculations. Moreover, the validity of the TB potentials under tension is discussed elsewhere [41] for a graphene sheet. Consequently, the Papaconstantpoulos TB potential is used in the analysis below.

The band structure of the (8,8) armchair CNT at $\varepsilon = 0.2$ evaluated by the TB calculation with the Papaconstantpoulos potential and by the ab initio calculations is shown in Fig. 3(a). The result by the TB calculation has small deviation from that by the ab initio one, but the band structure is well evaluated on the whole. The deviation is also small in the case of (9,0) tube (Fig. 3(b)). These results suggests that the electronic properties of CNTs under tension can be estimated by the TB calculations.

4. Electronic property of CNT under tension

4.1. Relaxation of atomic configuration and its effect on electronic structure

We conducted a tensile simulation to examine the effect of the relaxation on atomic and electronic structures by the tight-binding molecular dynamics calculation for the (8,8) armchair CNT model. The tensile strain, ε, is imposed by uniform stretching of the cell in the z direction. The atomic configuration is then relaxed by the molecular dynamics procedure where the kinetic energy is removed at certain steps.

Fig. 4 shows change in the atomic configuration of the (8,8) armchair CNT under 20% strain. Atomic configuration without and with relaxation after the application of tensile strain are illustrated by large and small circles, respectively, in the figure. There exists only a slight difference between them. Fig. 5(a) shows the electronic structures of these configurations, clearly indicating that the relaxation has little effect not only on the atomic structure, but also on the electronic one. The same verification is conducted for the (9,0) tube (Fig. 5(b)), which indicates that the effect of the relaxation is also negligible. This means that ignoring atomic relaxation does not greatly affect the result of atomic and electronic structures during axial tension of CNTs. Thus, in the following sections, we evaluate the electronic properties of CNTs under tension ignoring atomic relaxation.

4.2. Metallic–semiconducting transition

The electronic structures of CNTs with various structures under axial strain are evaluated by tight-binding calculations. The chiral vectors indicating the CNT structures used in the simulations are lis-

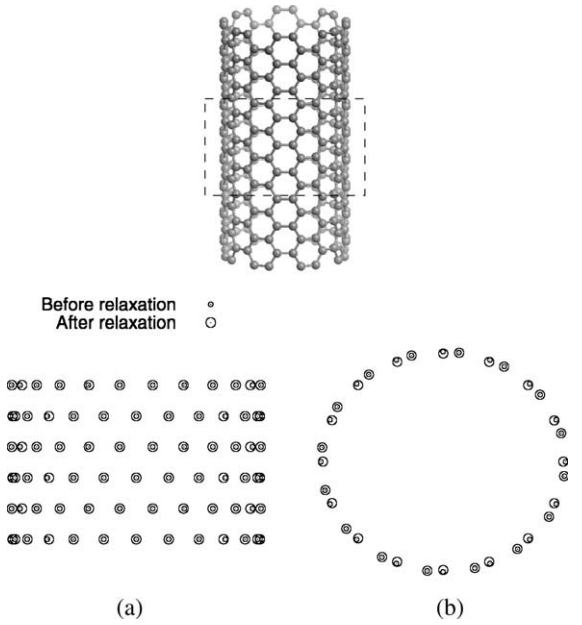

Fig. 4. Relaxation of atom configuration of (8,8) armchair CNT under tension. (a) Side view and (b) top view.

ted in Table 1. Axial tensile strain is imposed by the uniform stretching of the initial atomic configuration ($\varepsilon = 0$) in the z direction without relaxation.

4.2.1. Change in density of states during tension

Fig. 6 shows change in the density of states of (8,8) armchair and (14,0) zigzag tubes during tension. The (8,8) armchair tube has no band gap at the strain of 0, which means that it possesses metallic electronic properties at the initial state. Interestingly, no band gap appears at all throughout the tensile deformation, indicating that the (8,8) armchair tube retains its metallic properties during tension. On the other hand, the zigzag tube has a band gap at the strain of 0, the gap disappears at $\varepsilon = 0.05$, re-emerging at $\varepsilon = 0.1$. This indicates that the tube, which is metallic at the initial state, becomes semiconducting and returns to the metallic state as the tensile strain increases.

Table 1
Chiral vectors and diameters of CNTs for tensile simulations

(m,n)	d (nm)	(8,2)	0.7175
(6,1)	0.5134	(8,3)	0.7711
(6,2)	0.5646	(9,0)	0.7046
(6,3)	0.6214	(10,0)	0.7829
(7,1)	0.5911	(10,1)	0.8248
(7,2)	0.6408	(10,2)	0.8718
(7,4)	0.7550	(12,0)	0.9395
(8,1)	0.6689	(14,0)	1.0960

4.2.2. Change in E_{gap} under axial tension of various CNT structures

In this section, we present the band gap energy, E_{gap}, of CNTs with various chiral structures under axial tension. We classify the tubes into three groups: (a) $m - n = 3q$, (b) $m - n = 3q + 2$, and (c)

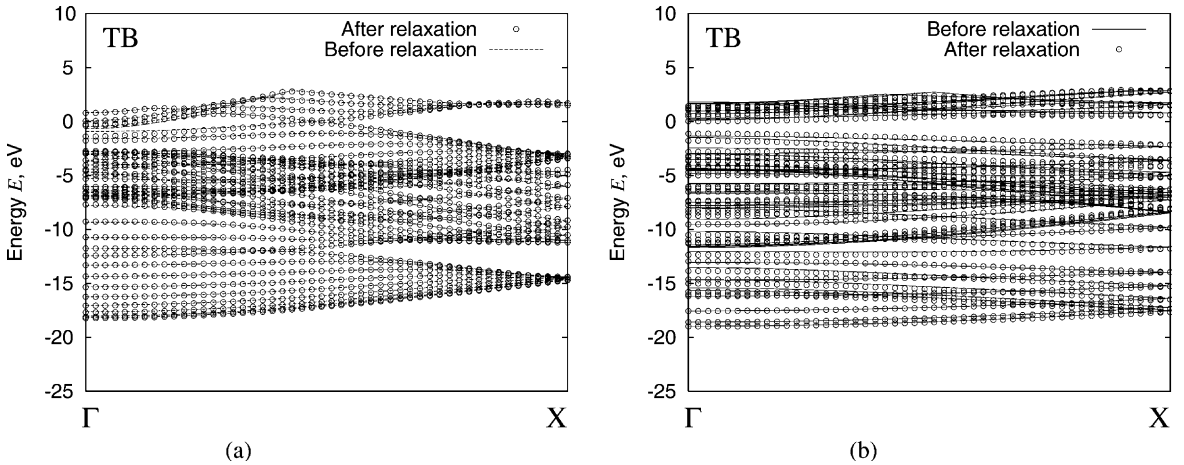

Fig. 5. Band structure of (8,8) and (9,0) CNTs under tension before and after relaxation ($\varepsilon = 0.2$). (a) (8,8) tube and (b) (9,0) tube.

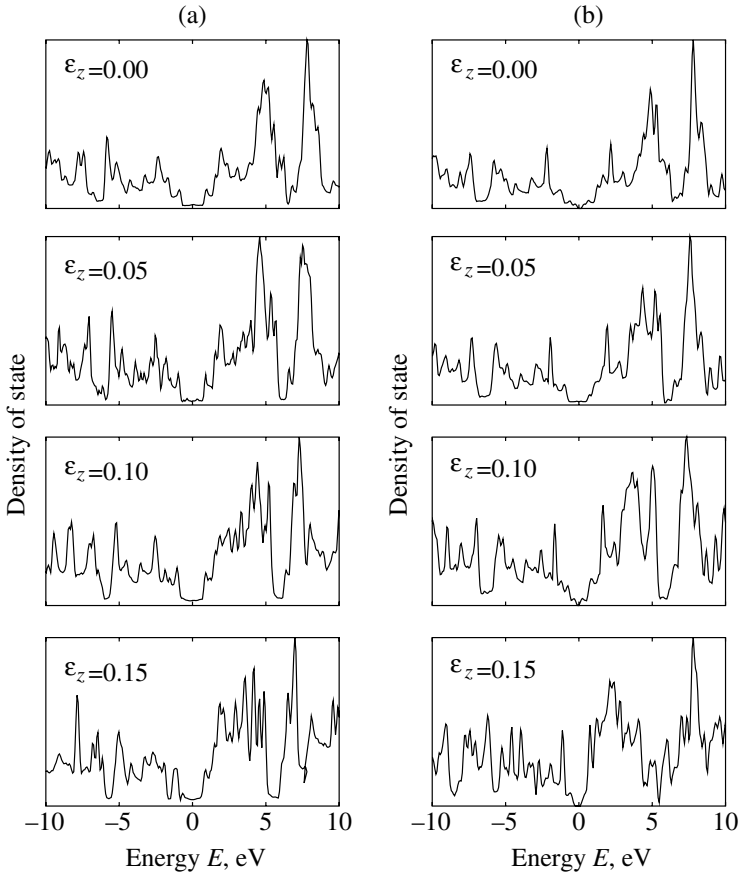

Fig. 6. Change in density of states of (a) (8,8) armchair and (b) (14,0) zigzag tubes during tension.

$m - n = 3q + 1$, where q is an integer. Here, armchair-type tubes are excluded since their electronic properties are metallic throughout axial tension, as mentioned in the previous section.

(a) $m - n = 3q$

Fig. 7 shows E_{gap} of CNTs with chiral vectors of $m - n = 3q$ during tension. E_{gap} is 0 at the initial state, $\varepsilon = 0$. When tensile strain is applied, a band gap appears in each CNT. The magnitude of tensile strain at which the band gap appears varies from 0.03 to 0.09, and as the tensile strain increases, E_{gap} temporarily increases before decreasing. E_{gap} becomes 0 again at high tensile strain. From the

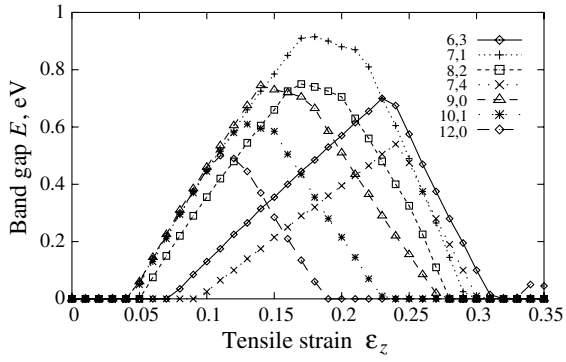

Fig. 7. Change in band gap energy of CNT with chiral vector of $m - n = 3q$ during tension.

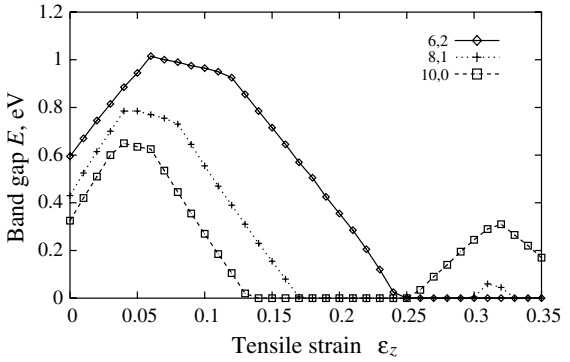

Fig. 8. Change in band gap energy of CNT with chiral vector of $m - n = 3q + 1$ during tension.

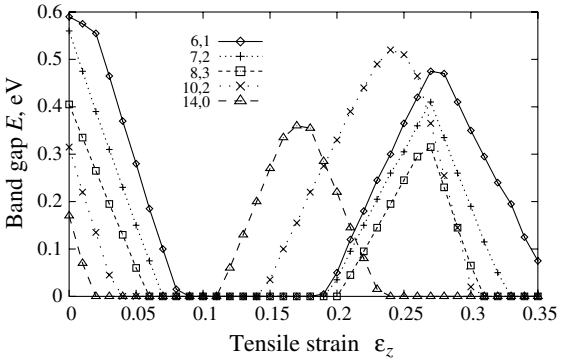

Fig. 9. Change in band gap energy of CNT with chiral vector of $m - n = 3q + 2$ during tension.

above results, we conclude that the CNTs change their electronic properties from metallic → semiconducting → metallic, as the strain increases. Moreover, the change appears at lower strain for CNTs with smaller diameters.

(b) $m - n = 3q + 1$

Fig. 8 shows change in E_{gap} of CNTs with chiral vectors of $m - n = 3q + 1$ during tension. The band gap at $\varepsilon = 0$ is positive and the tube with a smaller diameter has a larger band gap energy [3]. E_{gap} increases in the region of low strain; however, as the strain increases, the magnitude of E_{gap} decreases, finally resulting in the band gap's elimination. A CNT with a larger initial band gap possesses higher critical strain where the gap disappears, and the CNTs become semiconducting again as the tensile strain increases.

(c) $m - n = 3q + 2$

As shown in Fig. 9, the property in $m - n = 3q + 2$ is similar to that in $m - n = 3q + 1$. The value of E_{gap} at $\varepsilon = 0$ is positive and its magnitude depends on the diameter. However, E_{gap} is reduced as the tensile strain increases and the band gap is eliminated. The transient strain is dependent on the diameter and is relatively small compared to those of $m - n = 3q + 1$. The tubes become semiconductors again under further tension. Fig. 10 summarizes the transition of the electronic property of the CNTs.

5. Conclusions

We investigated changes in the electronic property of CNTs under high axial strain by performing tight-bindnig semiempirical band calculations after verifying the validity of the method in terms of evaluating the electronic property by comparison with ab initio calculations. The results obtained are summarized as follows:

(1) The band structure of (8,8) armchair CNT is calculated with the TB and the ab initio methods. The results agree closely with each other, which means that TB methods on the basis of appropriate selection of TB potentials give valid evaluations of the electronic properties of CNTs.
(2) Rearrangement of the atomic configuration under tension is small, thus the effect of relaxation can be neglected when evaluating the electronic properties of CNTs.
(3) Except in armchair tubes, the property of the CNTs with the chiral vectors of $m - n = 3q$(a) shows the transition: metallic → semiconducting → metallic, under tension. Armchair tubes

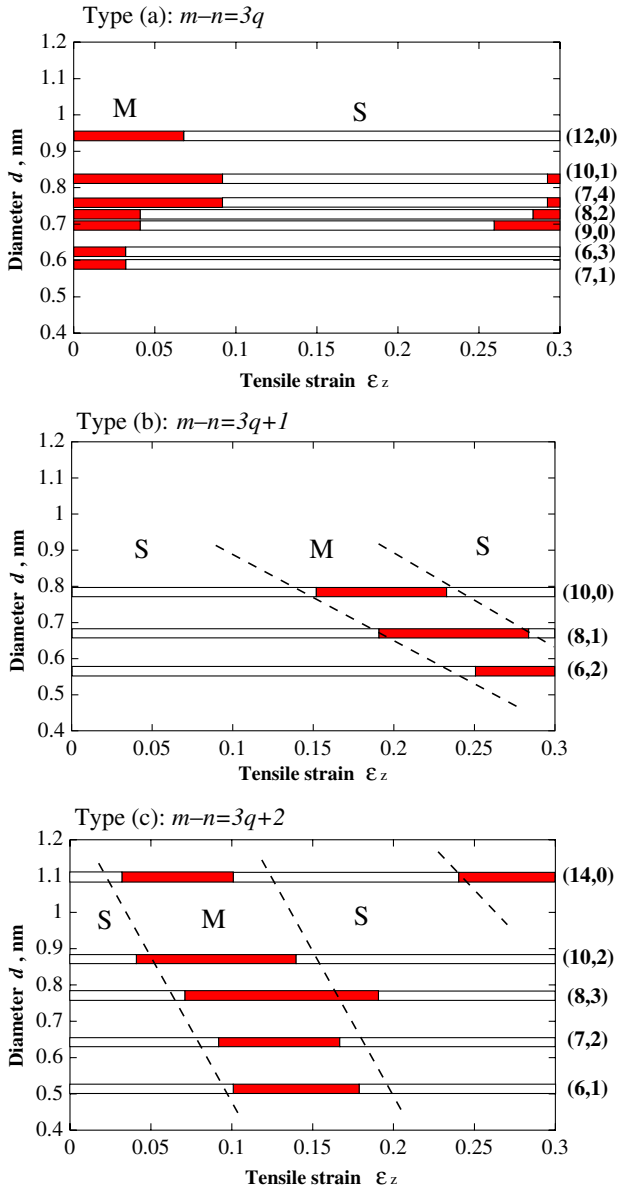

Fig. 10. Schematic illustrations explaining transition of electronic property of CNT. S and M in the figure indicate "semiconducting" and "metallic", respectively.

remain metallic throughout the period of tension.

(4) The transition of CNTs with the chiral vectors of $m - n = 3q + 1$(b) or $3q + 2$(c) is: semiconducting → metallic → semiconducting.
(5) In Types (b) and (c), the transient strain is dependent on the diameter of the CNTs.

Acknowledgements

This study was partly supported by the Asahi Glass Foundation, Industrial Technology Research Grant Program from New Energy and Industrial Technology Development Organization (NEDO), and a Grant-in-Aid for Scientific Re-

search (B) (No. 14350055) from the Japan Society of the Promotion of Science.

References

[1] S. Iijima, Nature 354 (1991) 56–58.
[2] S. Iijima, J. Appl. Phys. 42 (1991) 5891.
[3] M.S. Dresselhaus, G. Dresselhaus, R. Saito, Solid State Commun. 84 (1992) 201–205.
[4] N. Hamada, S. Sawada, A. Oshiyama, Phys. Rev. Lett. 68 (1992) 1579–1581.
[5] K. Tanaka, K. Okahara, M. Okada, T. Yamabe, Chem. Phys. Lett. 191 (1992) 469–472.
[6] R. Saito, M. Fujita, G. Dresselhaus, M.S. Dresselhaus, Appl. Phys. Lett. 60 (1992) 2204–2206.
[7] R. Saito, M. Fujita, G. Dresselhaus, M.S. Dresselhaus, Phys. Rev. B 46 (1992) 1804–1811.
[8] X. Blase, L.X. Benedict, E.L. Shirley, S.G. Louie, Phys. Rev. Lett. 72 (1994) 1878–1881.
[9] K. Okaraha, K. Tanaka, H. Aoki, T. Sato, T. Yamabe, Chem. Phys. Lett. 219 (1994) 462–468.
[10] K. Tanaka, H. Ago, Y. Yamabe, K. Okahara, M. Okada, Int. J. Quant. Chem. 63 (1997) 637–644.
[11] L. Yang, M.P. Anantram, J. Han, J.P. Lu, Phys. Rev. B 60 (1999) 13874–13878.
[12] L. Yang, J. Han, Phys. Rev. Lett. 85 (2000) 154–157.
[13] L. Yang, J. Han, M.P. Anantram, R.L. Jaffe, Comput. Model. Eng. Sci. 3 (2002) 675–685.
[14] S. Ogata, Y. Shibutani, Phys. Rev. B 68 (2003) 165409.
[15] G.B. Adams, O.F. Sankey, J.B. Page, M. O'Keeffe, D.A. Drabold, Science 256 (1992) 1792–1795.
[16] D. Robertson, D. Brenner, J. Mintmire, Phys. Rev. B 45 (1992) 12592–12595.
[17] A.A. Lucas, P.H. Lambin, R.E. Smally, J. Phys. Chem. Solids 54 (1993) 587–593.
[18] J.P. Lu, Phys. Rev. Lett. 79 (1997) 1297–1300.
[19] B.I. Yakobson, C.J. Brabec, J. Bernholc, Phys. Rev. Lett. 76 (1996) 2511–2514.
[20] M.S. Dresselhaus, G. Dresselhaus, A. Phaedon (Eds.), Carbon Nanotubes: Synthesis, Structure, Properties and Applications, vol. 291, Springer-Verlag, Berlin Heidelberg, 2001.
[21] D. Sánchez-Portal, E. Artacho, J.M. Soler, Phys. Rev. B 59 (1999) 12678–12688.
[22] E. Hernández, C. Goze, P. Bernier, A. Rubio, Phys. Rev. Lett. 80 (1998) 4502–4505.
[23] E.W. Wong, P.E. Sheehan, C.M. Lieber, Science 277 (1997) 1971–1974.
[24] M.R. Falvo, G.J. Clary, R.M. Taylor II, V. Chi, F.P. Brooks Jr., S. Washburn, R. Superfine, Nature 389 (1997) 582–584.
[25] M.F. Yu, O. Lourie, M.J. Dyer, K. Moloni, T.F. Kelly, R.S. Ruoff, Science 287 (2000) 637–640.
[26] D. Qian, G.J. Wagner, W.K. Liu, M.F. Yu, R.S. Ruoff, Appl. Mech. Rev. 55 (2002) 495–533.
[27] S. Ogata, Y. Shibutani, Phys. Rev. B 68 (2003) 165409.
[28] B.I. Yakobson, M.P. Campbell, C.J. Brabec, J. Bernholc, Comput. Mater. Sci. 8 (1997) 341–348.
[29] P. Hohenberg, W. Kohn, Phys. Rev. 136 (1964) B864–871.
[30] W. Kohn, L.J. Sham, Phys. Rev. 140 (1965) A1133–1138.
[31] J.C. Slater, G.F. Koster, Phys. Rev. 94 (1954) 1498–1524.
[32] A.P. Sutton, M.W. Finnis, D.G. Pettifor, Y. Ohta, J. Phys. C 21 (1988) 35–66.
[33] R. Car, M. Parrinello, Phys. Rev. Lett. 55 (1985) 2471–2474.
[34] K. Ohno, K. Esfarjani, Y. Kawazoe, Computational Materials Science: From Ab Initio to Monte Carlo Methods, vol. 77. Springer, 1999.
[35] N. Troullier, J.L. Martins, Phys. Rev. B 43 (1991) 1993–2006.
[36] D.M. Ceperley, B.J. Alder, Phys. Rev. Lett. 45 (1980) 566–569.
[37] J.P. Perdew, A. Zunger, Phys. Rev. B 23 (1981) 5048–5079.
[38] G. Kresse, J. Furthmüller, Phys. Rev. B 54 (1996) 11169–11186.
[39] M.J. Mehl, D.A. Papaconstantopoulos, Phys. Rev. B 54 (1996) 4519–4530.
[40] M.S. Tang, C.Z. Wang, C.T. Chan, K.M. Ho, Phys. Rev. B 53 (1996) 979–982;
M.S. Tang, C.Z. Wang, C.T. Chan, K.M. Ho, Phys. Rev. B 54–15 (1996) 10982, Erratum.
[41] A. Kushima, Y. Umeno, T. Kitamura, Proc. of Meso-Mechanics 2003: International Conferences on Computational Mesomechanics Associated with Development and Fabrication of Use-specific Materials.